the magnitude of the rolling moment, it is estimated that a rolling moment coefficient of 0.001 produces a steady rate of roll of about 3 deg/s. Taking this value as the acceptable error, the results show satisfactory agreement between the exact and single-point method predictions except close to the tanker wake downstream of its wing tip vortex, where the velocity gradient is high, and downstream of the wing trailing-edge kink, where a significant change in the spanwise gradient of the wing loading and downwash occur.

A similar conclusion applies to the prediction of the other aerodynamic parameters, namely, the induced drag, pitching moment, side force, yawing moment, and pitch angle. In the case of the side force and yawing moment, the present single-point analysis extends the planar expressions of Etkin[2] to include two components of the wake rate of roll. These are

$$P_{1w} = \frac{\partial W_w}{\partial y}, \qquad P_{2w} = \frac{\partial V_w}{\partial z} \tag{5}$$

The additional term P_{2w} relates to the variation in sidewash across the fin. Applying P_{1w} to all of the lifting surfaces, namely, wing, fin and tailplane, results in errors in the side force and yawing moment of up to 30% in the present case.

Further calculations, not presented in this Note, have shown that the single-point model of the receiver is essentially restricted to cases where the ratio of the receiver wing span to the tanker wing span is much less than one. An alternative multipoint model is, therefore, required for other practical cases of interest such as the refueling of a tanker aircraft in flight from another tanker aircraft. Span ratios vary from 0.91 in the case of a Hercules tanker refueling from a VC10 tanker to 1.12 in the case of a Tristar tanker refueling from a VC10 tanker. The single-point model, however, is considered adequate in simulating typical approaches of the Tornado combat aircraft to the hose and drogue trailing either from the centerline hose drum unit or the wing-mounted pod of the VC10 tanker. Although the single-point model is less accurate near the tanker wing tip vortex, this is of little concern because the combat aircraft would not be expected to fly in this region, and in any case, the combat aircraft would roll quickly on entering the tip vortex with the lift force displacing the aircraft sideways away from the tip vortex. For training purposes it may be useful to demonstrate this effect.

The validity of the exact vortex lattice method that equates the rotation of the leading aircraft vortex wake to variable downwash and sidewash over the following aircraft lifting surfaces has been investigated by Rossow.[7] Lift and rolling moment measurements were taken on a series of models of varying wing span located downstream of a B-747 aircraft model and traversed through the tip vortices. The data were then compared with results from the vortex lattice method using measured downwash distributions in the wake of the B-747 aircraft model as input to the vortex lattice code. Three following wings of span 0.19, 0.51, and 1.02 times the span of the wake-generating model were tested, and Rossow[7] found that the predicted loads on the following wings are reliable as long as the span of the following wing is less than 0.2 times the generator span. As the span of the following wing increases above 0.2, the vortex lattice method continues to predict correctly the trends and nature of the induced loads, but it overpredicts the magnitude of the loads by increasing amounts. Rossow[7] concludes that the wake of the generating wing is sufficiently altered by the large following wing to account for the discrepancy between theory and experiment. For the case considered in this Note, the wing span ratio is 0.30, although the wake interaction effect is less severe than that of Rossow[7] with the receiver located below the tanker tip vortex.

Conclusions

An approximate single-point model of the receiver aircraft in air-to-air refueling has been adapted from the planar aircraft model of Etkin[2] for flight in non-unform wind. The model is simple and easy to apply and has been validated in the case of the Tornado combat aircraft refueling from a VC10 tanker aircraft. Acceptable accuracy is achieved using the single-point model in all regions of the tanker wake except close to the tanker wake downstream of the wing tip vortex although this limitation is of little practical concern.

The single-point model becomes less accurate as the span of the receiver aircraft is increased and is unsuitable for cases involving large receiver aircraft such as a tanker refueling from another tanker.

Acknowledgments

The work reported here was carried out under a Defence Establishment Research Agency (DERA) research agreement and forms part of the DERA, Bedford program on the flight simulation of air-to-air refueling. The authors appreciate the guidance given by the staff of the Flight Management and Control Department at DERA, Bedford, particularly John Burnell, John Green, and John Keirl. The work is sponsored by the Ministry of Defence.

References

[1] Etkin, B., "Turbulent Wind and Its Effect on Flight," *Journal of Aircraft*, Vol. 18, No. 5, 1981, pp. 327–345.

[2] Bloy, A. W., and West, M. G., "Interference Between Tanker Wing with Roll-Up and Receiver Aircraft," *Journal of Aircraft*, Vol. 31, No. 5, 1994, pp. 1214–1216.

[3] Bloy, A. W., and Trochalidis, V., "The Performance and Longitudinal Stability and Control of Large Receiver Aircraft During Air to Air Refuelling," *Aeronautical Journal*, Vol. 93, No. 930, 1989, pp. 367–378.

[4] Krasny, R., "Computation of Vortex Sheet Roll-Up in the Trefftz Plane," *Journal of Fluid Mechanics*, Vol. 184, 1987, pp. 123–155.

[5] Etkin, B., and Etkin, D. A., "Critical Aspects of Trajectory Prediction: Flight in Non-Uniform Wind," AGARDograph 301, Vol. 1, 1990.

[6] Lea, K. A., "Aerodynamics of Air-to-Air refuelling," Ph.D. Dissertation, Univ. of Manchester, Manchester, England, U.K., 1995.

[7] Rossow, V. J., "Validation of Vortex-Lattice Method for Loads on Wings in Lift-Generated Wakes," *Journal of Aircraft*, Vol. 32, No. 6, 1995, pp. 1254–1262.

Studies on Vortex Flaps Having Different Flap Hinge-Line Positions

Kenichi Rinoie* and Dong Youn Kwak†
University of Tokyo, Tokyo 113-8656, Japan

Introduction

THE leading-edge vortex flap is a deflectable surface at the leading edge of a delta wing. A leading-edge separation vortex is formed over the flap surface, which helps to reduce the drag and to improve the lift/drag (L/D) ratio of the delta wing.[1] Many studies have confirmed the benefit of the vortex flap.

There are several factors that affect the vortex flap characteristics: first, sweepback angle of the delta wing; second, leading-edge shape, i.e., sharp or rounded leading edge; and third flap hinge-line position. The first author has carried out experimental studies using delta-wing models that have different sweepback angles fitted with tapered vortex flaps.[2] The benefit of the vortex flap was confirmed, and the effect of the sweepback angle was revealed. The first author also conducted wind-tunnel studies to determine the effect of the second factor, i.e., the difference between sharp and rounded leading-edge vortex flaps.[3] It was shown that deflecting the rounded leading-edge vortex flaps improves the L/D at relatively higher lift coefficients when compared with the sharp-edged vortex flaps.

Presented as Paper 2000-3.10.4 at the 22nd International Council of the Aeronautical Science Congress (ICAS), Harrogate, United Kingdom, 28 August–1 September 2000; received 8 October 2000; revision received 7 November 2000; accepted for publication 7 November 2000.

* Associate Professor, Department of Aeronautics and Astronautics, 7-3-1 Hongo, Bunkyo-ku. Member AIAA.

† Research Student; currently Research Fellow, Advanced Technology Aircraft Project Center, National Aerospace Laboratory, 6-13-1 Osawa, Mitaka, 181-0015, Japan.

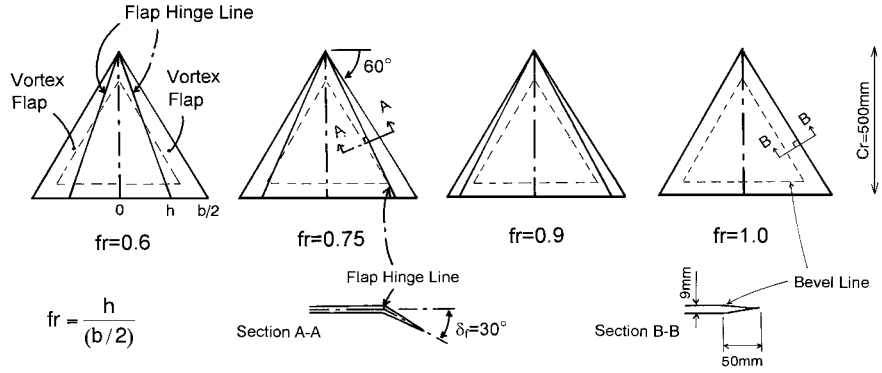

Fig. 1 60-deg delta-wing model with different *fr*.

The third factor, the effect of the vortex flap hinge-line position (i.e., spanwise length of the vortex flap) is investigated in this paper. The relationship between the spanwise length of the leading-edge separation vortex and that of the vortex flap plays an important role in the performance of the vortex flap. Therefore, wind-tunnel tests using 60-deg delta wing models with four different flap hinge-line positions were conducted.

Experimental Details

Figure 1 shows details of the delta-wing models. The 60-deg flat-plate delta-wing models with sharp leading edges that have four different flap hinge-line positions were used. The centerline chord length Cr is 0.5 m. The thickness of the model is 0.009 m. The upper and lower surfaces of all of the edges are beveled. The delta wing has vortex flap hinge lines running from the wing apex to the trailing edge. The vortex flap deflection angle δ_f is defined as the angle measured in the plane normal to the hinge line. The flap hinge-line position fr is defined as

$$fr = h/(b/2)$$

where h is the length between the flap hinge line and the wing centerline at the trailing edge and $b/2$ is the semispan length at the trailing edge. As for the plain delta wing without vortex flaps, fr equals 1. Models having $fr = 0.6$, 0.75, 0.9, and 1.0 were tested. Flap configurations of $\delta_f = 30$ deg were tested.

The experiments were carried out in the 2-m-diam open test section of the Gottingen-type wind tunnel at the University of Tokyo. All of the tests were performed at a tunnel speed of $U_\infty = 20$ m/s. The Reynolds number based on the wing centerline chord Re_{Cr} was 6.7×10^5. The models were suspended by wires from a three-component balance. The lift, drag, and pitching moment were measured using this balance. The wire tare drag effect was taken into account, and the tunnel boundary corrections were applied to the measured data. The angle of attack α was increased from -5 to 20 deg. Because of the tunnel balance geometry, angles of attack greater than 20 deg could not be used. All aerodynamic coefficients were based on the same datum wing area ($fr = 1.0$, i.e., plain delta wing). Flow-visualization tests using surface oil flow were conducted to describe the surface flow patterns. The estimated overall accuracy of the aerodynamic coefficients is $\pm 3\%$ at 20:1 odds.

Experimental Results

The measured lift coefficient C_L showed that the C_L decreases as fr decreases, that is, as the vortex flap area increases at constant α. The C_D–α curves showed that the C_D decreases for most of the positive α region, as fr decreases. These trends in C_L and C_D are similar to those when δ_f is increased at constant fr as are reported in Refs. 1–3. In Refs. 2 and 3 the delta-wing models that have $fr = 0.75$ flap hinge lines were tested.

Figure 2 shows the L/D vs C_L. A large L/D improvement for $\delta_f = 30$ deg is seen over the C_L range of 0.15 to 0.5. The maximum L/D is attained when $fr = 0.9$. However, the benefit of $fr = 0.9$ is only seen for the C_L range between 0.2 and 0.25. When $C_L > 0.25$,

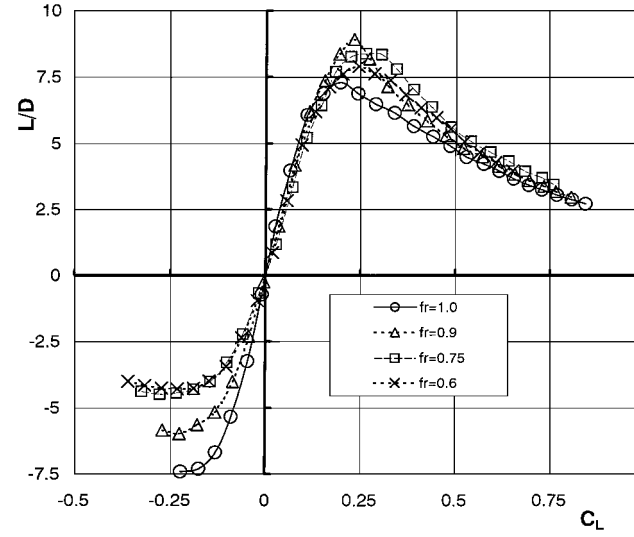

Fig. 2 L/D vs C_L for different *fr*.

$fr = 0.75$ indicates the best performance. Although all of the configurations ($fr = 0.9$, 0.75, and 0.6) show benefit in the L/D when compared with $fr = 1.0$ wing (plain delta wing), it is seen that the $fr = 0.6$ wing is the least effective. Reference 4 reported the effect of vortex flap hinge-line positions for a 60-deg delta wing when the $fr = 0.5$ and 0.75. The results indicated that the $fr = 0.5$ wing is less effective than the $fr = 0.75$ wing.

Figure 3 shows the surface flow patterns sketched from oil flow tests of the upper surface of the right wing at $\alpha = 8$, 10 and 12 deg for $fr = 0.75$ and 0.6. The patterns define the vortex positions on the wing and flap surfaces. In these figures HL denotes the flap hinge line. The hatched region denotes a small separation bubble, in which the oil moved very little. At $\alpha = 8$ deg for both the $fr = 0.75$ and 0.6 wings, there are only small separation bubbles (hatched regions) at the leading edge of the flap and at the flap hinge line. The flow attaches on the flap surface without any large separation. At $\alpha = 10$ deg for $fr = 0.75$, a leading-edge separation vortex is formed. Near the apex the vortex reattaches inboard of the flap hinge line. Near the trailing edge the chordwise length of the vortex reduces, and the vortex reattaches on the flap surface. At $\alpha = 12$ deg for $fr = 0.75$, the reattachment of the vortex occurs inboard of the hinge line for all chordwise stations. On the other hand, for the $fr = 0.6$ wing reattachment of the leading-edge separation vortex occurs over the flap surface at both $\alpha = 10$ and 12 deg.

Figure 4 shows the crossflow patterns plotted against α and fr. Flow patterns are deduced from the surface oil flow tests. The wing configuration, when the L/D attains its local maximum for a constant fr, is shown by the symbol *. This figure shows that the flow in crossflow planes can be divided into four different regimes. First, [in regime (A)] the leading-edge separation vortex is not formed, and only a small separation bubble is formed at the leading edge or

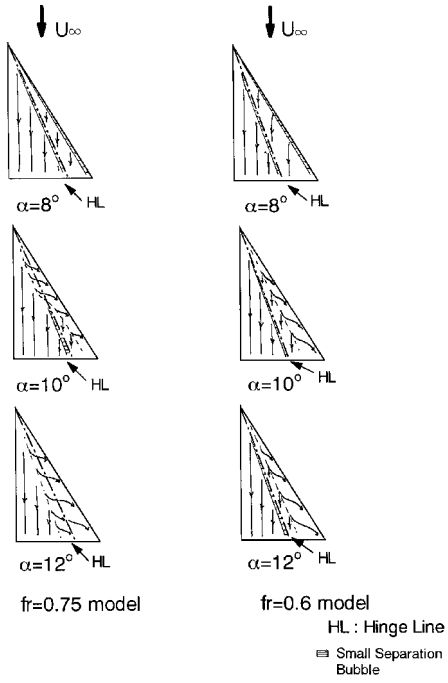

Fig. 3 Surface oil flow patterns at $fr = 0.75$ and 0.6.

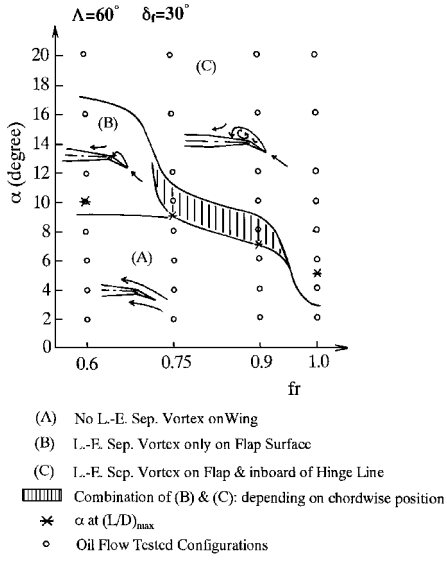

Fig. 4 Crossflow patterns for different fr.

at the flap hinge lines (at low α, all fr). Second, in regime (B) the leading-edge separation vortex is formed only over the flap surface (at $\alpha = 10$–16 deg, $fr = 0.6$ only). Third, in regime (C) the large separation vortex is formed, and its reattachment line is located inboard of the flap hinge lines (at high α, all fr). Finally, there is a fourth regime, a combination of regimes (B) and (C), in which the reattachment of the vortex occurs on the flap surface near the wing apex, but the reattachment occurs inboard the flap hinge line near the trailing edge, as was seen in Fig. 3 (at about $\alpha = 10$ deg, $fr = 0.75$ and 0.9). Figure 4 shows that the formation of a leading-edge separation vortex for the plain delta wing ($fr = 1$) is seen at $\alpha > 3$ deg for the first time when α is increased from 0 deg. However, once the flap is deflected, even though its spanwise length is only 10% ($fr = 0.9$), the angle of attack when the vortex is formed for the first time is $\alpha = 7$ deg. This indicates that a large change of flow pattern occurs even when a vortex flap that has small spanwise length is deflected ($fr = 0.9$). This may be related to the fact that the maximum L/D was attained for the $fr = 0.9$ wing when C_L was relatively small, as was shown in Fig. 2. The spanwise length of the vortex flap should be designed not only from the view point of aerodynamics but also from the results of wing structural studies.

Conclusions

In this note the effect of flap hinge-line positions over the performance of the leading-edge vortex flaps has been discussed. Differences of the vortex flap hinge-line position affect the performance of the vortex flap. The best L/D ratio is attained when the delta wing has vortex flaps with a relatively small spanwise length. The formation of leading-edge separation vortex over the wing is suppressed at relatively low angle of attack, even when the vortex flap with only a small spanwise length is deflected.

Acknowledgments

The authors express their gratitude to Y. Sunada and M. Morioka for their help in performing the wind-tunnel tests.

References

[1] Rao, D. M., "Leading Edge Vortex-Flap Experiments on a 74 deg. Delta Wing," NASA CR-159161, Nov. 1979.

[2] Rinoie, K., Fujita, T., Iwasaki, A., and Fujieda, H., "Experimental Studies of a 70-Degree Delta Wing with Vortex Flaps," *Journal of Aircraft*, Vol. 34, No. 5, 1997, pp. 600–605.

[3] Rinoie, K., "Experiments of a 60-Degree Delta Wing with Rounded Leading-Edge Vortex Flaps," *Journal of Aircraft*, Vol. 37, No. 1, 2000, pp. 37–44.

[4] Ellis, D. G., and Stollery, J. L., "The Behaviour and Performance of Leading-Edge Vortex Flaps," *Proceedings of 16th Congress of the International Council of the Aeronautical Sciences*, (ICAS Paper 88-4.5.2) 1988, pp. 758–765.

Performance Improvements of a Biplane with Endplates

N. A. Ahmed* and R. D. Archer†
University of New South Wales, Kensington, New South Wales 2052, Australia

Nomenclature

C_D = total drag coefficient of wing
C_L = lift coefficient of wing
e = span efficiency factor
Re = Reynolds number of flow based on wing chord, wind-tunnel airstream velocity, density, and dynamic viscosity
α = angle of attack or incidence

Introduction

HUMANKIND'S dream of powered flight became a reality when, in 1903, the Wright brothers demonstrated that high lift and structural rigidity of the biplane was essential to lifting man and engine into the air. However, with improvements in structural materials and technology, decreasing specific engine weights, and higher flight speeds, designers began to opt for the monoplane configuration.

In recent times, to meet the demands of an ever increasing air-cargo and transportation market, integration of any new aircraft into existing airports is becoming a significant consideration. The need for faster and more efficient aircraft with increased load carrying

Received 12 September 2000; revision received 17 November 2000; accepted for publication 26 November 2000.

*Senior Lecturer, Aerospace Engineering.
†Professor, Aerospace Engineering. Senior Member AIAA.